Self-archived version of the article published in Desalination:
M. Micari, M. Moser, A. Cipollina, A. Tamburini, G. Micale, V. Bertsch
Towards the Implementation of Circular Economy in the Water Softening Industry: A Technical, Economic and Environmental Analysis, Journal of Cleaner Production, 255, 2020, 120291. https://doi.org/10.1016/j.jclepro.2020.120291

Towards the Implementation of Circular Economy in the Water Softening Industry: A Technical, Economic and Environmental Analysis

M. Micari[1]*, M. Moser[1], A. Cipollina[2], A. Tamburini[2]*, G. Micale[2], V. Bertsch[1,3]

1 German Aerospace Center (DLR), Institute of Engineering Thermodynamics, Pfaffenwaldring 38-40, 70569 Stuttgart, Germany

2 Dipartimento di Ingegneria, Università degli Studi di Palermo (UNIPA), viale delle Scienze Ed. 6, 90128 Palermo, Italy

3 Ruhr-Universität Bochum, Lehrstuhl Energiesysteme und Energiewirtschaft (LEE), Universitätsstr. 150, 44801 Bochum, Germany

*corresponding authors: alessandro.tamburini@unipa.it; marina.micari@dlr.de

Abstract

In this work, we propose an integrated methodological approach aimed at identifying the most suitable strategy to improve the sustainability of the water softening industry via the treatment and recycling of the produced wastewater. For the first time, different concentration technologies and energy supply systems are compared to minimize the environmental impact of the industrial process and to ensure the economic feasibility of the treatment system. The comparison concerns three treatment chains, presenting the same pre-treatment step (nanofiltration and crystallization) and different concentration technologies: Multi-Effect Distillation (MED), Membrane Distillation (MD) and the coupling of Reverse Osmosis and Membrane Distillation (RO-MD). In the case of electricity supplied by the grid, the MED and the RO-MD chain are economically competitive with the state of the art (Levelized Brine Cost (LBC) between 4 and 6$/m^3, lower than the regenerant solution cost, equal to 8$/m^3). Moreover, the specific CO_2 emissions due to the energy required by the treatment processes (10.8 $kg_{CO2}/m^3_{regenerant}$ for the MED chain and 16.7$kg_{CO2}/m^3_{regenerant}$ for the RO-MD chain) are lower than those produced by the current system (19.7$kg_{CO2}/m^3_{regenerant}$). Varying the feed flow rate, the MED-chain is more feasible at larger plant sizes for its lower energy demand, while the chain including RO-MD shows lower costs at smaller plant sizes for its lower

investment costs. When a photovoltaic-battery system is coupled, both the MED-chain and RO-MD-chain show a CO_2 emission reduction of more than 75% with respect to the state of the art. Furthermore, their LBC values are very competitive, especially if the plant is located in a region with high solar potential.

Keywords

Industrial Wastewater, Circular Economy, Treatment chain, CO_2 emissions, Recycling, Membrane Processes

1. Introduction

Sustainable development (SD) is considered the only feasible answer to the simultaneous growth of energy and water demand and the increase in environmental pollution. According to the definition given by the Brundtland commission in 1987, SD is able to "*meet the needs of the present without compromising the ability of future generations to meet their own needs*" (World Commission on Environment and Development 1987). SD is typically presented as a three-dimensional concept, which accounts for environmental, social and economic aspects. Therefore, different criteria may be employed to assess the sustainability of a process, such as CO_2 emissions, water and energy requirements, costs, labour conditions and economic growth (Janeiro and Patel 2015). One of the most acknowledged ways to achieve the SD consists in the application of the circular economy (CE) concept (Geissdoerfer et al. 2017). The concept was originally introduced by Boulding in 1966 and suggests that economy should be a circular system to ensure the sustainability of human life on Earth (Boulding and Jarrett 1966). According to the definition given by the Ellen MacArthur Foundation, CE is "*an industrial economy that is restorative and regenerative by intention and design*" (Ellen MacArthur Foundation 2013). The main objective of CE is the promotion of a more appropriate and environmentally friendly management of resources, to achieve a *cleaner industrial production* (Ghisellini et al. 2016). To this aim, new business models (Gusmerotti et al. 2019) and, eventually, a redesign of the industrial processes (Zhijun and Nailing 2007) are required to decouple the economic growth and the consumption of resources (Suárez-Eiroa et al. 2019). Different methodologies and indicators are used to assess the CE performances: most methods concern Life Cycle Assessment analyses and process design to enable the circularity (Sassanelli et al. 2019). The indicators, which were proposed in 2018 by the European Commission within a CE monitoring framework, mostly concern circularity degree, waste generation and production of secondary raw materials (Eurostat 2018). These

can be categorized according to the levels of application: *micro* (single processes or consumers), *meso* (industrial parks) and *macro* (cities, regions or nations) (Saidani et al. 2019).

Several works in literature focused on the implementation of CE at the micro-level, investigating new strategies to treat the industrial effluents and to produce (i) sellable raw materials and/or (ii) material streams to be reused in the industrial process. Significant attention has been devoted to the food industry (Mirabella et al. 2014). Depending on the specific food, different types of waste are produced and consequently different substances may be extracted (Cardinali et al. 2012), (Abdelkader et al. 2019). The sugar industry produces a significant amount of waste and the investigated waste valorisation strategies mostly regard the utilization of sugarcane biomass for energy (Gopinath et al. 2018) and biofuels production (Cardona et al. 2010). Also in textile industry, the production of wastewater streams represents a severe issue, because of the high content of colour, organic compounds and salt in the discharged dyeing solution (Holkar et al. 2016). Different strategies have been developed to treat and recycle the effluent as fresh dyeing solution: these include combinations of membrane processes, as ultrafiltration and nanofiltration (Nadeem et al. 2019), advanced oxidation processes (Bilińska et al. 2017) and biological treatments (Sarayu and Sandhya 2012). Finally, other industrial sectors are characterized by high water consumption and, consequently, by the production of significant volumes of wastewaters, such as paper, laundering and coal mine industry. To achieve a sustainable production, the wastewater may be treated to reduce the organics content (Man et al. 2017) and to recover valuable materials, as water and detergent in the laundering industry (Giagnorio et al. 2017) and salts (Turek et al. 2008) as well as rare earth elements in the coal mine industry (Lopez et al. 2019).

Another industrial process producing significant volumes of wastewater is the water softening industry. Water softening is a purification process aimed at removing the hardness from water, via the employment of Ion Exchange resins. Periodically, the resins are regenerated supplying a NaCl-water solution and the regeneration produces a wastewater stream, containing sodium, chloride and bivalent ions (magnesium, calcium and sulphate ions). Currently, this effluent is disposed into the environment, since there are no organic pollutants or harmful components. However, the frequent release of concentrated brine from Na-charged softeners is becoming a crucial concern as it is detrimental to agriculture and downstream water quality (Li et al. 2016). A few works in the literature focused on the design of alternative ion exchange resins (Li et al. 2016), (Birnhack et al. 2019) or alternative thermal

(Chandrasekara and Pashley 2015) and electrochemical regeneration processes (Chen et al. 2016) to avoid the release of a high amount of Na^+. However, in most cases, the technical investigation is not coupled with an economic and environmental analysis of the proposed systems.

This work focuses on proposing and demonstrating a methodological approach for the identification of the most suitable treatment chains to achieve a *cleaner* production in the industrial water softening, integrating technical, economic and environmental analyses. The proposed treatment chains are devised to reduce the demand of raw materials in the industrial process and to limit the environmental pollution due to the effluent disposal. In fact, in the proposed configurations, the Na-rich effluent is not disposed into the environment, as it is treated and then recycled to the industrial process. The chains present a pre-treatment and a concentration step, as shown in Figure 1. The pre-treatment processes (nanofiltration and crystallization) aim at separating the bivalent ions, while in the concentration steps the remaining NaCl-water solution is concentrated up to the concentration of the fresh regenerant solution to be recycled. Three alternative concentration technologies are considered: (i) multi-effect distillation (MED), (ii) membrane distillation (MD) and (iii) reverse osmosis coupled with membrane distillation (RO-MD).

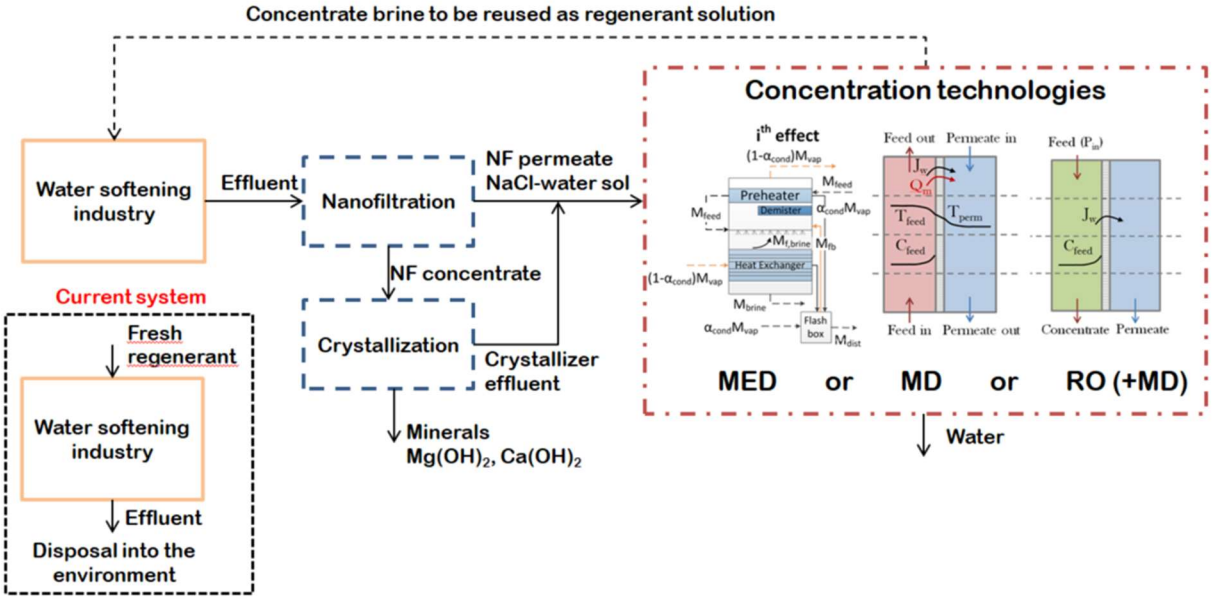

Figure 1. Scheme of the treatment chains for the presented case study. The industrial process is represented by the box framed in yellow (solid line), the pre-treatment steps by the ones in blue (dashed line) and the concentration step alternatives in red (dash-dotted line). The box on the left (black dotted line) represents the current industrial process.

Firstly, the chains with different concentration technologies are compared, by assessing the economic feasibility, the energy requirements and the environmental impact due to the CO_2 emissions. Secondly, we investigate the impact of different drivers on the selected technologies, with a focus on the self-generation of electricity via a PV-battery system and on the solar radiation conditions of the region selected for the plant location.

Overall, for the first time, this work aims at establishing a methodological approach that allows for identifying the most economically feasible and environmentally friendly strategy to move towards a CE approach in the water softening industry, comparing different concentration technologies and energy supply systems.

2. Methodological Approach

The methodological approach followed in this work is sketched in the block diagram of Figure 2. This novel multi-step approach provides various levels of investigation. Firstly, techno-economic models are developed and implemented for each process on the basis of literature equations, experimental data and data given by the vendors. Secondly, the most significant technical and economic inputs and outputs of the models are defined and, accordingly, the models are interconnected. Different systems can be devised depending on how the models are interconnected and, correspondingly, different treatment chains can be simulated. Finally, for a given set of operating conditions and input data, the performance of each chain is estimated via the definition of global outputs, accounting for technical, economic and environmental aspects.

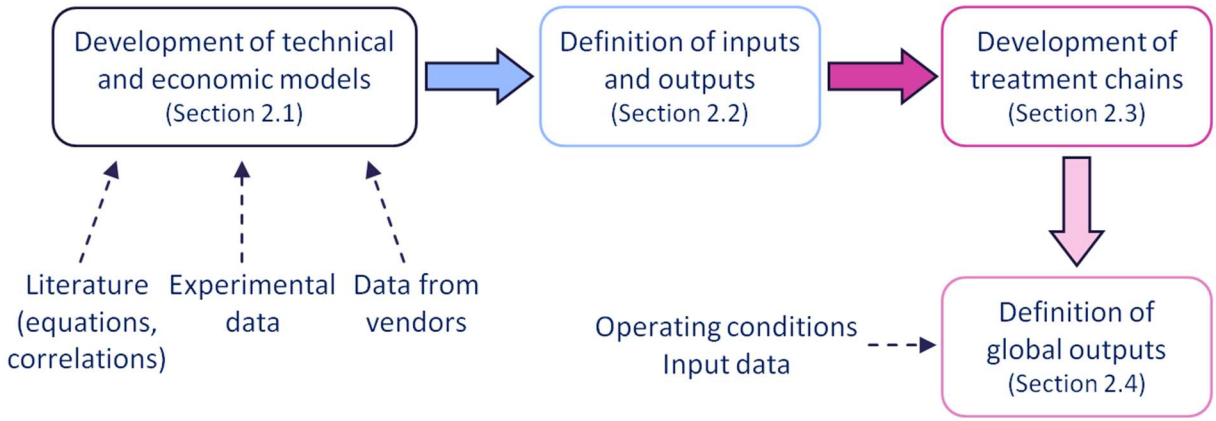

Figure 2. Block diagram showing the methodological approach followed in this work.

2.1 Development of technical and economic models

In the following, a short description of the techno-economic models is reported. The models of NF and MED were described in previous works (Micari et al. 2019a, Micari et al. 2019b) and RO and MD models are presented in the Supplementary Materials.

Nanofiltration.

Nanofiltration is a pressure-driven membrane process, which is suitable to remove bivalent and multivalent ions thanks to the high membrane rejection.

We implemented a multi-scale model including three different scales. The *low-hierarchy model* assesses the membrane behaviour and is based on the Donnan Steric Pore Model with Dielectric Exclusion (Geraldes and Brites Alves 2008). The model solves the extended Nernst-Plank equation within the thickness of the membrane and takes into account the boundary conditions given by the exclusion mechanisms (Labban et al. 2017). The main results of the low-hierarchy model are the ionic rejections and the water flux. These are some of the inputs of the *medium-hierarchy model*, which describes the NF unit along the feed main flow direction. Thus, mass balances are applied to define the concentration and flow-rate of permeate and feed for each discretization step (Roy et al. 2015). Finally, the *high-hierarchy model* estimates the required size of the NF plant, given by NF units arranged in series and in parallel, to achieve a certain total recovery (ratio between permeate and feed flow-rates). Regarding the energy demand, the NF process requires electricity to pump the feed up to the defined pressure. The economic model follows the Verberne cost model (Van der Bruggen et al. 2001).

Crystallization.

Two crystallization units are included in the chains to produce $Mg(OH)_2$ and $Ca(OH)_2$, using a NaOH-water solution as alkaline reactant. Each crystallizer is followed by a filter, where the crystals are obtained from the magma produced in the crystallizer. For this process, we implemented a simplified model based on mass balances under the assumption of a 100% conversion of the dissolved Mg^{2+} and Ca^{2+} into $Mg(OH)_2$ and $Ca(OH)_2$ respectively (Cipollina et al. 2014). Concerning the energy demand, two terms are estimated: (i) the pumping energy to pump the solutions to the crystallizers and (ii) the electric energy required by the filters. Finally, regarding the economic model, the Module Costing Technique is applied for the estimation of the capital costs, with suitable parameters for crystallizers and filters found in literature (Turton et al. 2012). The operating costs are due to the reactant and the energy supply, while the revenues are given by the minerals, which are supposed to be sold at the current market price.

Multi-Effect Distillation.

The MED process has been widely investigated in literature, mostly for seawater desalination purposes (Kamali et al. 2008), (El-Dessouky and Ettouney 1999). The MED plant modelled for this work presents a forward-feed arrangement, since this is more suitable to the high temperatures and concentrations expected in the investigated cases (Ortega-Delgado et al. 2017). The plant is composed of a certain number of stages in series, each one presenting a heat exchanger, where the feed partially evaporates, and a preheater, where the feed is heated up before entering inside the stage. The model includes an iterative procedure, which runs until three conditions are simultaneously achieved: (i) the areas of the heat exchangers of each stage are equal, (ii) the areas of the preheaters are equal and (iii) the outlet distillate flow-rate fulfils the overall mass balances, depending on the required brine concentration. The distillate is supposed to be pure water, which can be sold at the current market selling price.

Concerning the energy requirements, the thermal energy is the prominent term, given by the steam flow-rate multiplied by the latent heat at the given pressure. The electricity demand is fixed and equal to 1.5kWh/m^3_{dist} (Gebel and Yuce 2008). The details of the economic model are reported in a previous work (Micari et al. 2019b).

Reverse Osmosis.

Reverse Osmosis is a desalination process, based on a membrane separation under an applied pressure. The model has a hierarchical structure, as shown in detail in the Supplementary Materials: it goes from the investigation of the membrane properties and the estimation of the fluxes to the design of a whole plant. The RO plant typically presents many vessels arranged in parallel to reach a certain total recovery, similarly to the NF plant (Dow Water and Process Solutions). Each vessel contains a number of RO units in series with spiral-wound geometry. Concerning the energy demand, RO requires only electricity to pump the feed up to the inlet pressure. Finally, the economic model includes the calculation of the capital costs, composed of the costs of membrane elements, pressure vessels, high pressure pumps, piping and intake costs (Wilf and Bartels 2005), (Malek et al. 1996). The operating costs account for electricity demand, maintenance (3%/y of the investment plus 20% of the annual labour cost), labour, chemicals and membrane replacement (Vince et al. 2008).

Membrane Distillation.

MD is a separation process, which presents a microporous hydrophobic membrane, permeable only to water vapour. A temperature gradient between the two membrane interfaces leads to a vapour pressure difference, which generates a vapour flux through the membrane. The present model describes a Direct Contact MD (DCMD) configuration, which was selected for its simplicity and the high vapour fluxes (Winter et al. 2011). The details of the implemented model are reported in Supplementary Materials. In the *DCMD membrane model*, the trans-membrane vapour flux is calculated combining heat and mass transfer equations (Qtaishat et al. 2008). In the *DCMD unit model*, mass and energy balances are set up to investigate flow-rate, concentration and temperature profiles along the feed stream-wise direction (Hitsov et al. 2017). Finally, the *DCMD plant model* simulates a high-scale plant, where the MD units are arranged in series and in parallel to reach a high recovery (Ali et al. 2018). Regarding the energy consumption, heat is required to increase the temperature of the feed from the intake to the inlet temperature and in each intermediate heater. Electricity is required to pump the feed and the permeate entering each module in series. The economic model estimates the capital costs, given by the costs of modules, membrane, pumps and heat exchangers, together with the cost for intake and pre-treatment (Hitsov et al. 2018). Conversely, the operating costs comprise the electricity and heat demand, maintenance (2.5%/y of the investment cost without the cost of membranes and modules), labour, chemicals and membrane replacement cost (Al-Obaidani et al. 2008).

2.2 Definition of inputs and outputs

Every treatment process presents inlet and outlet material and energy flows, which correspond to inputs and outputs of the technical models. Most of the outputs generated by the technical models are fundamental for costs' estimation. The most important inputs and outputs for each model are reported in Table 1, where the outputs constitute the inputs for the relevant economic model.

Table 1. Main inputs and outputs of the technical models.

MODEL	INPUTS	OUTPUTS
Nanofiltration (NF)	- Feed flow-rate and composition - Feed pressure - Total recovery - N° of elements (vessel) - Membrane rejection	- Permeate flow-rate and composition - Retentate flow-rate and composition - N° of vessels in parallel - Electricity demand
Crystallization (cryst)	- Feed flow-rate - Feed concentration (Mg^{2+} and Ca^{2+}) - Alkaline solution concentration	- Produced flow-rate of hydroxides - Flow-rate of alkaline solution - Effluent flow-rate and composition - Electricity demand
Reverse Osmosis (RO)	- Feed flow-rate and concentration - Retentate outlet concentration - N° of stages and of elements (vessel)	- Permeate flow-rate and composition - Retentate flow-rate - N° of vessels in parallel - Electricity demand
Membrane Distillation (MD)	- Feed flow-rate and concentration - Retentate outlet concentration - Inlet feed and permeate temperatures - Intake temperature	- Distillate and retentate flow-rate - N° of elements (series and parallel) - Heat and electricity demand
Multi-Effect Distillation (MED)	- Feed flow-rate and concentration - Retentate outlet concentration - N° of effects - Steam temperature	- Area of heat exchangers - Steam flow-rate - Heat and electricity demand

2.3 Development of the treatment chains

The techno-economic models are integrated and interconnected in a simulation platform called Remote Component Environment (RCE) (https://rcenvironment.de/). Figure 3 shows the workflow generated to simulate the chain with RO-MD (NF-cryst-RO-MD). The blocks corresponding to the processes call the relevant models and exchange data (e.g. the NF retentate concentration and flow-rate constitute the concentration and flow-rate of the crystallizer feed). Analogous workflows are built for the other two chains, with MED (NF-cryst-MED) and with MD (NF-cryst-MD).

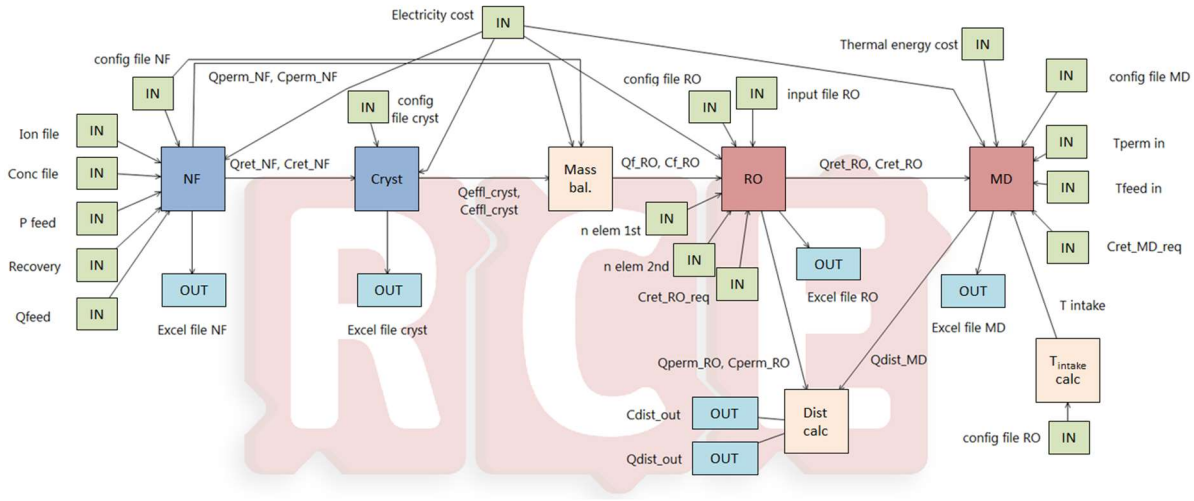

Figure 3. Workflow of the NF-cryst-RO-MD chain as implemented in RCE. The dark-blue blocks represent the units in the pre-treatment step and the red blocks the units in the concentration step; the green units the input values or files; the light blue blocks the outputs; the light orange blocks the intermediate tools (mixing units). (Q: flow-rate; C: concentration; P: pressure; T: temperature)

2.4 Definition of global outputs

To properly compare the treatment chains, we defined some representative output parameters, relevant to the technical, economic and environmental performances of the whole system. Concerning the technical aspects, the heat and electricity demands [kW] have been adopted as reference outputs. Regarding the economic analysis, the total annualized capital costs (CAPEX [$/y]) and the total operating costs (OPEX [$/y]) are the most significant parameters for each unit. For each treatment chain, a levelized cost is used, which represents the price at which the main product of the chain should be sold to break-even and which includes all the capital and operating expenses of the units and the revenues coming from the by-products. In the present case, the main product is the concentrate brine (Q_{brine}) which can be reused as a reactant in the industrial process and a global parameter called Levelized Brine Cost (LBC_{tot} [$\$/m^3_{brine}$]) is taken as the reference economic output (Micari et al. 2019b). The LBC_{tot} is given by the combination of the terms relevant to the capital costs (LBC_{cap}) and to the operating costs and the revenues (LBC_{op}).

$$LBC_{tot} = LBC_{cap} + LBC_{op} = \\ = \frac{\sum_{units} CAPEX}{Q_{brine}} + \frac{\sum_{units} OPEX - Revenue_{Mg(OH)_2} - Revenue_{Ca(OH)_2} - Revenue_{water}}{Q_{brine}} \quad (1)$$

Finally, regarding the environmental aspects, all chains allow minimizing the direct discharge of effluent into the environment, which, instead, occurs in the current system. Another important aspect consists in the CO_2 emissions due to the heat and electricity supply. In the present work, we focused only on the operational CO_2 emissions, as these resulted to be much higher than the ones due to the construction of desalination plants (Liu et al. 2015). The CO_2 emissions per m^3 of produced brine [kg_{CO2}/m^3_{brine}] are used to compare the different chains and to compare each chain with the current system.

3. Description of case study and scenarios

The general methodological approach described in Section 2 has been developed to be flexible and applicable to different case studies. In the present work, we followed this approach to identify the most suitable treatment chain for the effluent produced by the regeneration of ion exchange resins employed for water softening. In this section, we present the case study and the scenarios investigated.

3.1 Description of the case study

The regeneration process producing the effluent is sketched in Figure 4. The effluent is given by the sum of the regenerant and the rinse solutions, which contribute to the outlet flow-rate with an approximate ratio of 1:9. Under the assumption of a continuous operation, a plant producing around 130m^3/h of effluent firstly receives the regenerant solution with a flow-rate of 13m^3/h and secondly receives pure water, as the rinse solution, with a flow-rate of 117m^3/h.

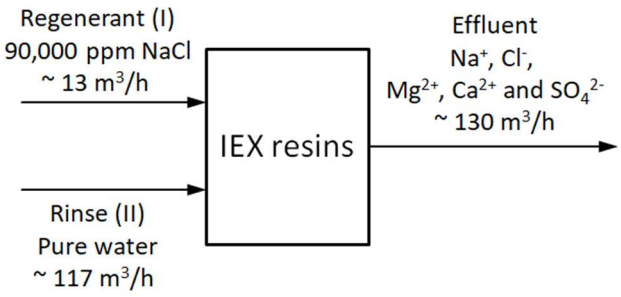

Figure 4. Schematic description of the IEX resins regeneration phase assuming a continuous operation.

The effluent contains sodium, chloride and bivalent ions removed from the spent resins during the regeneration process. The composition of the wastewater produced by a real water softening plant located in Rotterdam, The Netherlands, is reported in Table 2.

Table 2. Composition of the effluent produced by the water softening process.

	C_{Na}	C_{Cl}	C_{Mg}	C_{Ca}	C_{SO4}
[mol/m^3]	173.9	662.2	55.6	191.7	3.1
[ppm]	3,892	22,556	1,298	7,462	292

The treatment chains are devised to produce a concentrate solution (brine) with a NaCl concentration equal to the one of the fresh reactant required by the regeneration process. Therefore, for any chain, the main constraint consists in the concentration of the produced brine (MED concentrate or MD retentate solution), which has to be equal to 90,000ppm. In the case of the RO-MD chain, firstly, the solution is concentrated up to 70,000ppm in the RO unit (this is the maximum achievable concentration in RO (Kesieme et al. 2013)) and then up to 90,000ppm in the MD unit.

Concerning the operating conditions, the NF plant operates with a feed pressure of 20bar and a recovery of 25% (Micari et al. 2019a). The membrane rejections are equal to 94.8% for Mg^{2+}, 83% for Ca^{2+}, 93.6% for SO_4^{2-}, -50.6% for Na^{+} and 49.9% for Cl^{-}, which are in line with values reported in literature (Zhou et al. 2015). The MED plant includes 13 stages, on the basis of a previous MED cost minimization analysis (Micari et al. 2019b) and the thermal energy is supplied in the form of vapour at a pressure of 1bar. The RO plant includes two stages (presenting 8 and 6 elements per vessel), since the recovery is between 50 and 70%. Finally, regarding the MD plant, the inlet feed and permeate temperatures are equal to 80°C and 20°C and each MD module presents 6 units wounded in parallel.

For the economic analysis, the capital costs are annualized by defining depreciation period and discount rate, while the operating costs depend on several factors, such as plant capacity and pumps' efficiency. These parameters, the specific costs of the utilities and the selling price of the products are reported in Table 3.

Table 3. Parameters used for the economic analyses.

Parameter	Value	Units
Discount rate	6	%
Units' life time (Straight line depreciation)	• NF, structure: 30 (Van der Bruggen et al. 2001) • NF, electrical and mechanical: 15 • Crystallizer: 20 • RO: 25 (Vince et al. 2008) • MED: 25 (Papapetrou et al. 2017) • MD: 10 (Hitsov et al. 2018) • PV and battery: 25	y
Capacity factor	0.94	-
Pumps' efficiency	0.8	-
Cost of electricity (grid)	0.103	$/kWh
Cost of thermal energy	0.01	$/kWh
Replacement rate of membranes	RO, MD: 15 (Al-Obaidani et al. 2008) NF: 20 (Van der Bruggen et al. 2001)	%/y
Price of $Mg(OH)_2$	1200 (U.S. Department of the Interior 2017)	$/ton
Price of $Ca(OH)_2$	300 (U.S. Department of the Interior 2017)	$/ton
Price/cost of water	1 (Mezher et al. 2011)	$/m3
Cost of NaCl for the regenerant solution (current technology)	80 (Micari et al. 2019b)	$/ton
Cost of PV modules	1000 (Fraunhofer ISE 2015)	€/kW
Cost of battery	400 (Breyer et al. 2017)	€/kWh
Cost of converter	200 (Breyer et al. 2017)	€/kWh

3.2 Definition of the scenarios

To assess the role of the electricity supply on the costs and the environmental impact, we defined *two scenarios*:

1. in the first, electricity is completely taken from the grid;
2. in the second, electricity is mostly supplied by a photovoltaic (PV) power system, with Li-Ion battery storage units operating in conjunction, while the remaining fraction of required electricity is taken from the grid. The PV technology has been chosen rather than the wind technology, because it is more modular and its power production is less uncertain compared to wind. The natural irregularity of wind requires implementation

of oversized batteries, which lead to much higher Levelized Cost of Electricity (LCOE) values.

Regarding the *first scenario*, we considered the current mix of electricity carriers of the grid in The Netherlands (since we are making reference to a real water softening plant located in Rotterdam), with the corresponding efficiencies and CO_2 emission factors, reported in Table 4. The combination of the emission factors of the single carriers, their efficiency and share of the electricity output gives rise to a global CO_2 grid intensity equal to 0.471kg_{CO2}/kWh.

Table 4. Electricity carriers' mix in the grid in The Netherlands in 2016: electricity output, efficiency and CO_2 emission factor for each carrier (International Energy Agency 2018), (IPCC 2006).

Electricity Carriers The Netherlands (2016)	**Electricity output [%]**	**Efficiency (total output) [-]**	**CO_2 emission factor [kg/kWh_{prim}]**
Hard Coal, coal products	37.69	0.42	0.335
Natural Gas	44.87	0.54	0.201
Biomass	4.45	0.34	-
Mineral oil product	1.27	1	0.27
Nuclear	3.72	0.33	-
Hydro	0.09	1	-
PV	1.00	1	-
Wind	6.90	1	-
Total	100		

Concerning the *second scenario*, the share of energy demand covered by the PV-battery system is estimated running an integrated model implemented in INSEL (Moser et al. 2014). More details are given in the Supplementary Materials. The produced power corresponds to a certain share of the total load, given by the electricity demand of the treatment chain in one year [MWh/y]. The plant is supposed to work in stationary operation conditions, therefore the total electricity demand is considered always constant. The remaining demand is supplied by the grid, with the electricity carriers' mix used in the previous scenario (Table 4). In this case, the CO_2 emissions are only due to the fraction of electricity supplied by the grid. Finally, the PV-battery system located in The Netherlands is compared with an analogous system located in one of the European regions with the highest solar potential, i.e. Valencia in Spain.

Concerning the costs, in the *first scenario* the current cost of electricity for non-household consumers is considered (Eurostat 2019). In the *second scenario* the cost is calculated as the combination of the LCOE due to the PV-battery system and the cost of electricity from the grid. Within the first term, the capital costs are given by the cost of the PV modules and the battery. The operating cost of the PV and the battery are calculated as 1.5%/y and 2.5%/y of the investment cost, respectively. Finally, within this scenario, in one case we assumed that no taxation is imposed on the CO_2 emissions, while in the other case we considered an average CO_2 price of 80 €/ton$_{CO2}$ (International Energy Agency 2018).

3.3 Overview of the performed analyses

Having defined the operating conditions and the scenarios, we carried out simulations varying technical (Q_{feed}), economic ($Cost_{El}$ and $Cost_{Heat}$) and environmental ($f_{CO2,emission}$) inputs. The overview of the analyses performed within the two scenarios is reported in Table 5.

Table 5. Summary of the analyses reported in the present work.

	Scenario	Variable input	Fixed inputs
Wastewater: spent IEX regenerant solution	Scenario 1. Electricity supply: grid only (Section 4.1)	Q_{feed} (10-150m^3/h) (Section 4.1.1)	$Cost_{El}$=0.103 \$/kWh $Cost_{Heat}$=0.01\$/kWh
		Q_{feed} and $Cost_{Heat}$ (different heat sources) (Section 4.1.2)	$Cost_{El}$=0.103 \$/kWh
	Scenario 2. Electricity supply: PV-battery-grid (Section 4.2)	$Cost_{El}$ and $f_{CO2,emission}$ (different PV-battery system configurations) (Sections 4.2.1 and 4.2.2)	Q_{feed}=130 m^3/h $Cost_{Heat}$=0.01\$/kWh

4. Results and Discussion

All analyses are performed applying the same circularity concept: the brine produced by the concentration step is recycled to the IEX resins as the fresh regenerant. Therefore, the target concentration of the brine is fixed for all cases and, consequently, on the basis of the global mass balances, its flow-rate is always around 40% of the effluent flow-rate. In other words, the chains are able to produce around 4 times the volume of solution required for

regeneration, thus they ensure the self-sufficiency for raw materials (i.e. the regenerant solution), which is one of the CE indicators provided by the European Commission. Moreover, the three chains present the same pre-treatment unit, which is able to recover more than 95% of dissolved Mg^{2+} and Ca^{2+} as $Mg(OH)_2$ and $Ca(OH)_2$. Finally, all chains are devised to allow the complete recycling of the effluent and to minimize the waste generation. Overall, the CE approach is analogous in the three chains, while the costs and the energy demands for its implementation depend on the processes and will be compared in the following sections.

4.1 Scenario 1. Electricity supply from the grid

In Scenario 1, electricity is supplied from the grid at a constant cost, which is the current cost of electricity for non-household consumers in The Netherlands, equal to 0.086€/kWh (0.103$/kWh in 2018).

4.1.1. Feed flow-rate variation

Firstly, the three chains are compared varying the inlet effluent flow-rate: this variation causes a variation of both capital and operating costs, since the required size of the plant and the energy consumption depend on the flow-rate. The trends of LBC_{cap} and LBC_{op} vs. the feed flow-rate are reported in Figure 5.

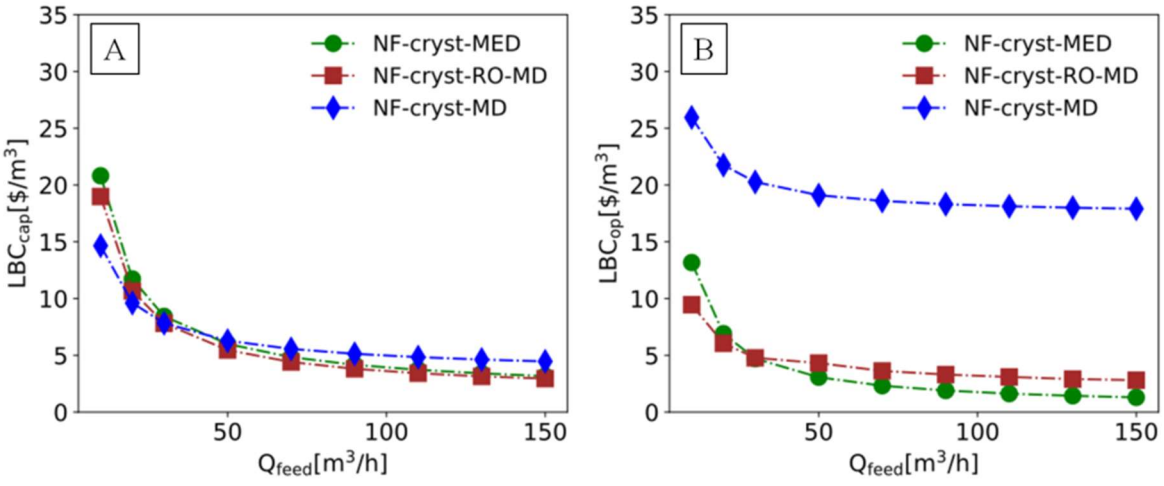

Figure 5. LBC_{cap} (A) and LBC_{op} (B) of the three chains (NF-cryst-MED, NF-cryst-RO-MD, NF-cryst-MD) as a function of Q_{feed} [m^3/h]. Grid supply, $Cost_{El}$=0.103$/kWh; waste heat, $Cost_{Heat}$=0.01$/kWh.

In agreement with economy of scale, for each system, the highest levelized cost is found at the lowest flow-rates, while much lower and slowly decreasing values are observable at high flow-rates (Figure 5A). At small scales, the plants with RO and MD show lower capital costs

with respect to the one with MED, since RO and MD are modular technologies, typically suitable to small scales. Conversely, at higher flow-rates, the gap between the LBC_{cap} of the RO-MD and the MED chain significantly decreases and the MD chain reports the highest LBC_{cap} because of the high number of required modules. The design flow-rate of each commercial MD module is fixed and defines the number of branches in parallel. Moreover, since the recovery of the single MD unit is thermodynamically low, it is necessary to arrange more modules in series and in particular, each branch in parallel presents 15 modules in series in the first stage and 8 in the second.

Regarding the operating costs (Figure 5B), at low flow-rates, the trends present an evident diminution, due to the variation of the maintenance costs, which depend directly on the investment costs. Conversely, at higher flow-rates, the profiles are almost constant, since most of the operating costs are due to the energy demand, which is linearly proportional to the feed flow-rate. Notably, the MD-chain operating costs are much higher than the others in the whole range of Q_{feed} because of the high MD thermal demand. The combination of LBC_{cap} and LBC_{op} (which includes the revenues coming from minerals and water production) gives rise to LBC_{tot}, reported in Figure 6.

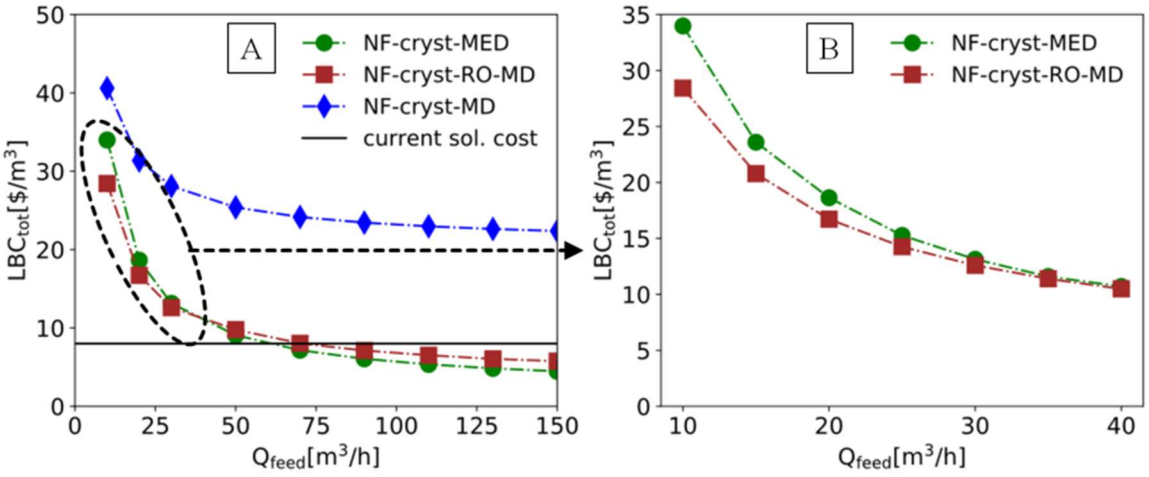

Figure 6. (A) LBC_{tot} of the three chains (NF-cryst-MED, NF-cryst-RO-MD, NF-cryst-MD) as a function of Q_{feed} [m^3/h] and (B) a zoom in the low flow rates region to compare NF-cryst-MED and NF-cryst-RO-MD chains. Grid supply, $Cost_{El}$=0.103$/kWh; waste heat, $Cost_{Heat}$=0.01$/kWh.

The comparison of the LBC_{tot} of the three systems highlights that the chains with MED and with RO-MD behave similarly, while the chain with MD shows much higher LBC_{tot} in the whole range of Q_{feed}, because of the crucial operating costs of MD. Interestingly, the curves of LBC_{tot} of the two most performing plants intersect at a feed flow-rate of around 40m^3/h (see the zoom in Figure 6B): at lower flow-rates the RO-MD plant is more convenient because of

its modularity which leads to lower investment costs, while at higher flow-rates the MED chain is more feasible thanks to the lower energy requirements. Finally, it is remarkable that in a very wide range of Q_{feed} (higher than 60m^3/h for the MED chain and higher than 70m^3/h for the RO-MD chain) the LBC_{tot} falls below the current cost of the fresh regenerant solution (Figure 6A). This implies that both chains are more economically convenient than the state of the art which provides a continuous supply of fresh reactant at a cost of 8$/$m^3$.

Furthermore, the total electricity and heat requirements of the three chains varying the feed flow-rate are reported in Figure 7.

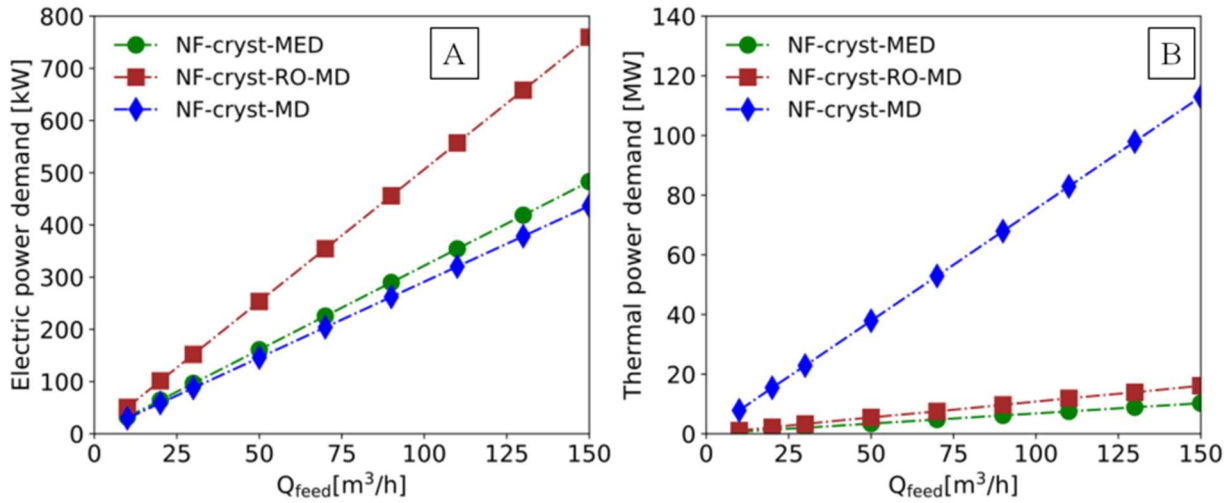

Figure 7. Electric (A) and thermal (B) power demand for the three chains varying Q_{feed}.

Firstly, in all cases, both electricity and heat demand show a linear trend, as expected. The RO-MD chain shows the highest electricity demand, since the RO unit is a pressure-driven process. Conversely, the MD-chain exhibits a significantly higher heat demand, because of the high MD specific thermal consumption (around 900kWh_{th}/m^3_{dist}). Moreover, in the RO-MD chain, MD leads to an increase of the thermal demand of the chain beyond that of the MED one, even if it is supposed to cover only a fraction of the concentration change (from 70,000ppm to 90,000ppm).

To compare our results with previous works, we calculated the system costs and the energy consumption per equivalent of hardness removed during regeneration (the removed hardness was calculated from the concentration of Mg^{2+} and Ca^{2+} in the effluent, shown in Table 2). For the case of a plant producing 130m^3/h of effluent, we found a cost 0.022$/$eq_{hardness}$ without the revenues coming from the by-products. For an alternative treatment system providing also the recycle of the NaCl regenerant solution, a previous work reported a cost of

0.172\$/$eq_{hardness}$ (Birnhack et al. 2019). Concerning the energy consumption, they presented a solely electricity-driven treatment process with a consumption of around 0.132$kWh_{el}/eq_{hardness}$. Our chain with MED shows lower values of electricity demand (~0.0062$kWh_{el}/eq_{hardness}$) but it requires also thermal energy (~0.138$kWh_{th}/eq_{hardness}$). However, it is difficult to perform an exact comparison, since the involved processes and the scale of the systems are different.
Finally, the environmental impact of the three chains is assessed looking at the CO_2 emissions due to the energy production. Since the thermal energy is supposed to be industrial waste heat, additional electricity is considered for pumping and compressing the heat. The guidelines report a default value of 0.09GJ of electricity required per GJ of heat recovered (Harmelink and Bosselaar 2013). Thus, this electricity demand is also accounted for the calculation of the CO_2 emissions. Figure 8 shows the CO_2 emissions due to the total energy demand of the three chains.

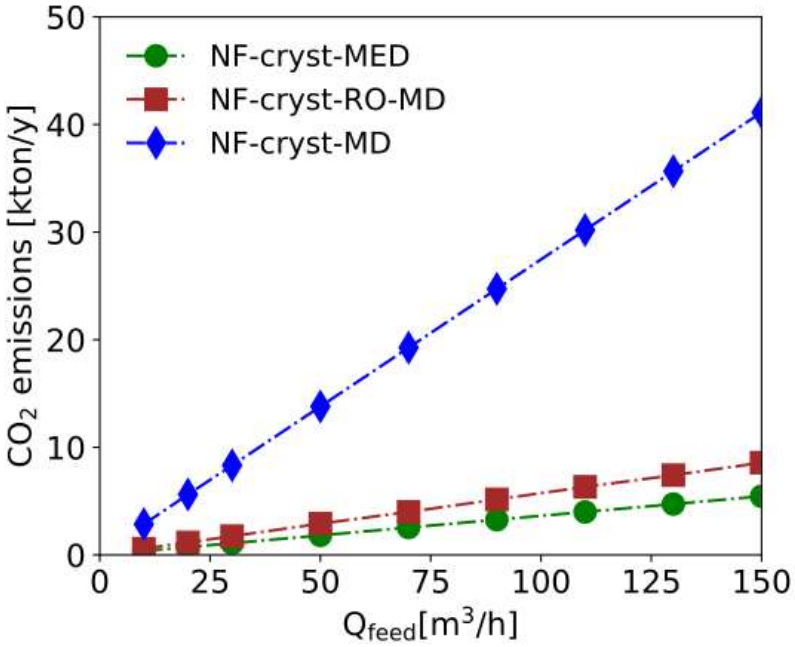

Figure 8. CO_2 emissions of the three chains, considering the current power generation mix from the grid and assuming a demand of 0.09GJ_{el} for each GJ of waste heat recovered.

Also from an environmental point of view, the MD-chain is the worst performing, because of its large energy demand. Conversely, the other two chains show lower emissions. To compare the CO_2 emissions of the chains with the current industrial process, it has to be considered that around 10,000ton/year of NaCl are required for the preparation of the regenerant solution with the flow-rates reported in Section 3.1. The NaCl production is very energy intensive: the electricity demand for salt crystallization by mechanical vapour recompression is

450kWh/ton$_{salt}$ (Sedivy 2006). The energy demand of the salt production process, considering the yearly requirement of salt in the plant, leads to around 2.1kton/y of CO_2 emissions. On top of this, the emissions due to the production of the demineralized water used for the preparation of IEX regenerant solution and the salt transportation should be accounted. However, these terms are too site-specific and, conservatively, have not been considered in this study. For comparison, we calculated the ratio between the CO_2 emission and the fresh regenerant (brine) flow-rate, which results equal to 19.7kg$_{CO2}$/m$^3_{brine}$ for the current system. In the proposed treatment schemes, the MED and the RO-MD chains treat the same flow rate of effluent (130m^3/h) and produce around 53m^3/h of brine solution, reusable as regenerant. The chains show global values of CO_2 emissions equal to 4.7 and 7.3kton/y respectively, which correspond to a ratio between the CO_2 emissions and the produced brine of 10.8 and 16.7kg$_{CO2}$/m$^3_{brine}$. Thus the CO_2 emissions can be reduced, with both chains, even considering the current energy mix of the grid.

4.1.2 Simultaneous variation of feed flow-rate and energy cost

To investigate also the role of the heat cost, we performed a simultaneous variation of feed flow-rate and thermal energy cost. Three heat sources are considered: industrial waste heat available in the site, gas turbine co-generation cycle and boiler burning natural gas. The relevant heat costs define a range, which goes from 0 up to about 0.07\$/kWh$_{th}$, in the case of the boiler where natural gas at a cost of 0.065\$/kWh is burnt with an efficiency of 90% (EIA 2019).

Figure 9 reports the contour-maps of LBC$_{tot}$ for the NF-cryst-MED and the NF-cryst-RO-MD chains varying feed flow-rate and heat cost. The NF-cryst-MD chain was not further analysed since it reported the worst results in all cases. The line in black collects all the points where LBC$_{tot}$ is equal to 8\$/m^3, which is the value used as a threshold, since it is the current cost of the regenerant solution. In both cases, the feasibility area, i.e. the region above the line, enlarges as Q_{feed} increases, since the levelized capital costs are lower and a higher expense for the thermal energy can be met within the feasibility region. Comparing the two technologies, the NF-cryst-RO-MD chain shows a smaller feasibility area and this is explicable considering its higher energy requirement. However, the minimum flow rate found in its feasibility region is lower (around 38m^3/h) and this demonstrates that the RO-MD system is more economically convenient in the case of smaller plant size. Overall, both systems show a significantly wide range of operating conditions where they result more competitive than the state of the art.

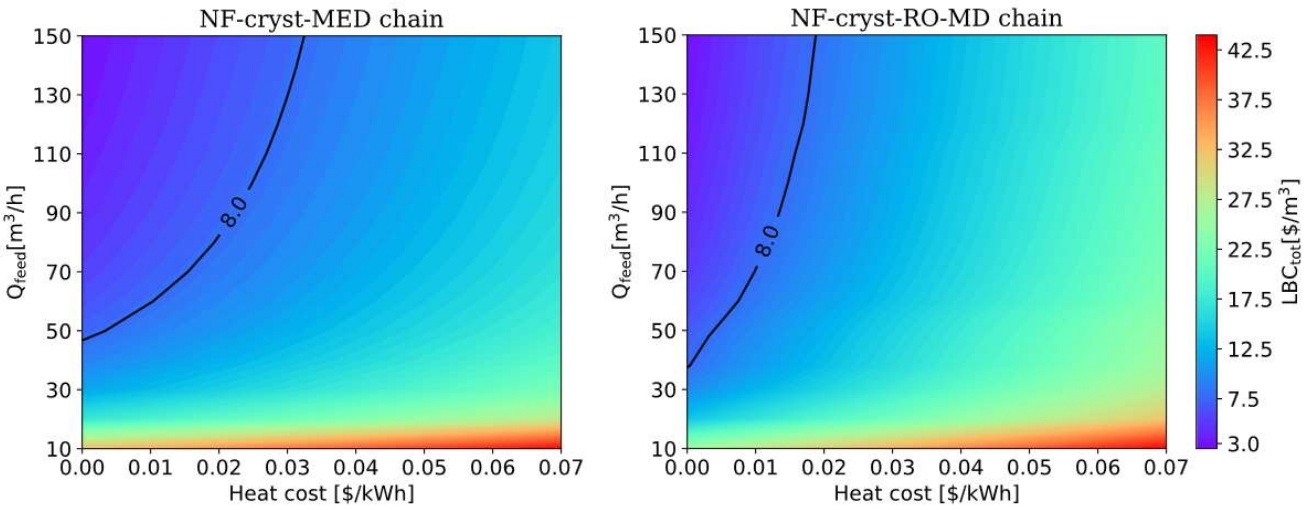

Figure 9. Heat maps of the LBC_{tot} of the NF-cryst-MED chain (left) and of the NF-cryst-RO-MD chain (right) varying Q_{feed}[m³/h] and $Cost_{Heat}$[$/kWh]. Grid supply, $Cost_{El}$=0.103$/kWh. Black line: LBC_{tot} equal to 8$/m³ (current cost of the fresh regenerant solution).

4.2 Scenario 2. Electricity supply from a PV-battery system

In Scenario 2, electricity is supplied by a dedicated PV-battery system. On the basis of the meteorological characteristics of the location, the electricity self-sufficiency (i.e. the share of the demand covered by the PV-battery system) is derived; the rest is taken from the grid, assuming the cost used in Scenario 1.

4.2.1 PV-battery system configurations: global LCOE and emission factors

Parametric analyses varying the installed PV power and the capacity of the battery give rise to a scatter of LCOE values as a function of the CO_2 emission factor. The configurations found in correspondence to the lower envelope of the scatter plots, shown in Figure 10, are used to define the LCOE values and the corresponding emission factors in Scenario 2. In chart A, the emissions are not subjected to taxation, while in chart B the CO_2 emissions are taxed with a price of 80€/ton. More details about the PV-battery system simulations are given in the Supplementary Materials.

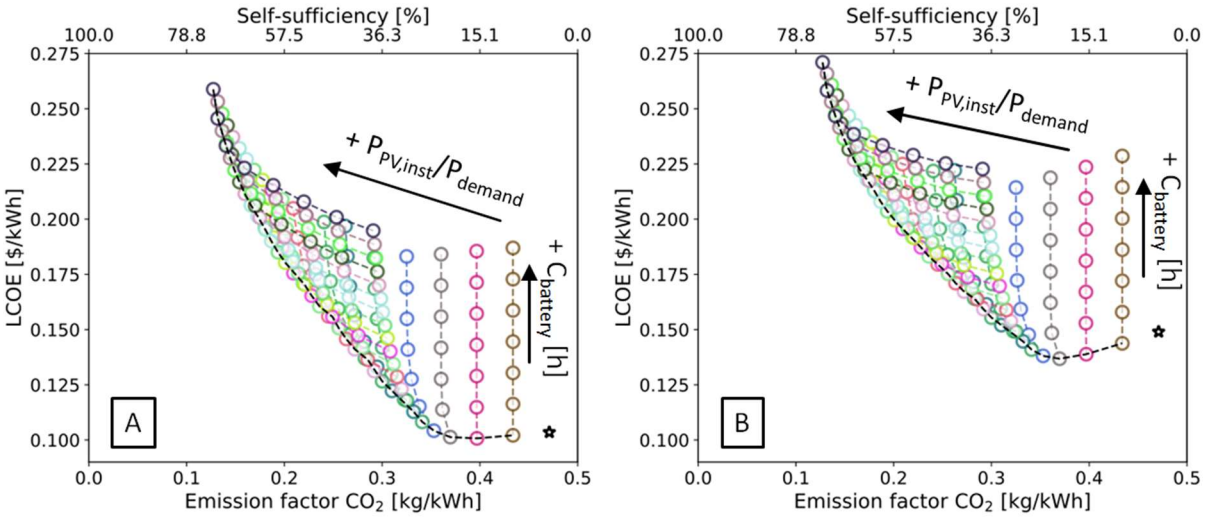

Figure 10. LCOE [$/kWh] of the PV-battery-grid supply as function of the CO_2 emission factor from the grid [kg/kWh] varying the P_{inst}/P_{demand} ratio from 0.5 to 10 (step of 0.5) and the full load hours of the battery from 0 to 17.5h (step of 2.5h). For Figure A no taxation on the CO_2 emissions is considered, while in Figure B the CO_2 emissions have a cost of 80€/ton_{CO2}. The asterisk symbol (*) indicates the grid supply point.

4.2.2 Treatment chains results

Figure 11A shows the trends of LBC_{tot} of the NF-cryst-MED and NF-cryst-RO-MD chains varying the LCOE within the ranges reported in Figure 10A and B. Notably, for each chain, the LBC_{tot} trends with or without the taxation on the CO_2 emissions are partially overlapped, since part of the estimated LCOE range is the same, even if in correspondence to different CO_2 emission factors (see Figure 10A and B). The two chains exhibit a linear trend of LBC_{tot} vs. LCOE, since the operating cost due to the electricity demand is the only varying term and it linearly depends on the given LCOE. Remarkably, even if the LCOE becomes more than two times the value of the electricity cost from the grid, the competitiveness of both chains is ensured almost in all cases: the MED chain presents values of LBC_{tot} much lower than the threshold in the full range of LCOE, while the RO-MD chain presents values of LBC_{tot} slightly higher than the threshold only for LCOE higher than 0.25$/kWh. Figure 11B shows how much the LBC_{tot} increases when the CO_2 emissions decrease, in correspondence to higher shares of renewables in the energy supply system. As expected, the difference between the cases with or without taxation becomes more evident when higher shares of electricity are taken from the grid. Finally, it is remarkable the difference in the CO_2 emissions between Scenario 1, represented by the star marker and the cases analysed in Scenario 2. Therefore, with a PV-battery system, it is possible to reduce dramatically the emissions and, at the same time, ensure the economic feasibility of both chains. In the case with CO_2 taxation, the most environmentally friendly and feasible systems are the MED chain with LBC_{tot} of 6.1$/$m^3_{brine}$

and CO_2 emissions of 2.9kg_{CO2}/m^3_{brine} and the RO-MD chain with LBC_{tot} of 7.9$/$m^3_{brine}$ and CO_2 emissions of 5.1kg_{CO2}/m^3_{brine}. Therefore, the MED chain ensures a CO_2 emissions reduction with respect to the current system of 85% and the RO-MD chain of 75%.

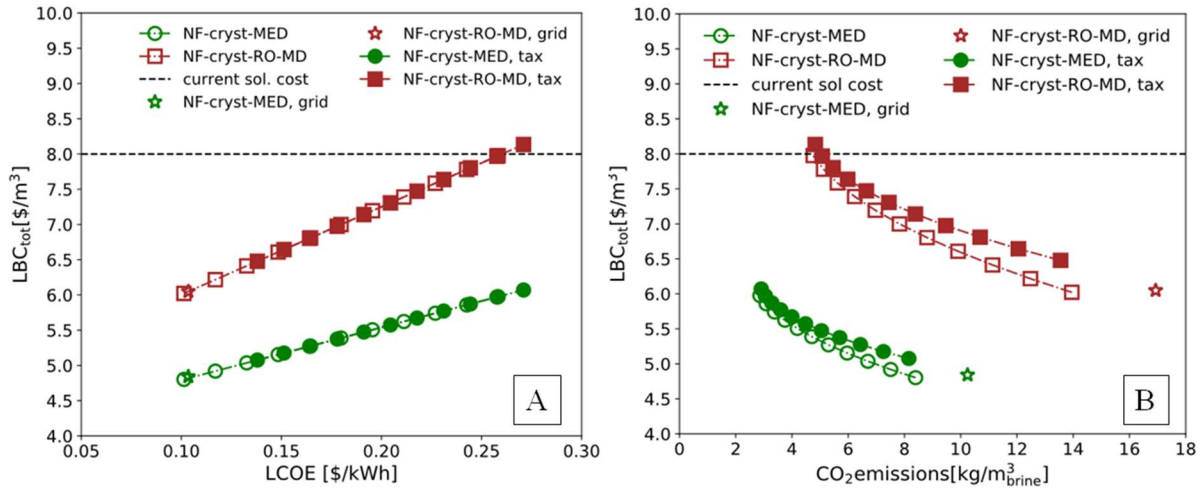

Figure 11. LBC_{tot} vs. LCOE (A) and LBC_{tot} vs. the CO_2 emissions (B) for the NF-cryst-MED and the NF-cryst-RO-MD chains, with and without taxation on the CO_2 emissions. The asterisk symbol (*) represents the cases of grid supply (Scenario 1).

4.2.3 Impact of the meteorological characteristics: comparison with a plant in Valencia, Spain

The analysis discussed above is performed also considering a different plant location: Valencia in Spain, which was selected since it is one of the European areas with the highest solar potential. Figure 12 shows the lower envelopes of the scatter plots of LCOE vs. CO_2 emission factor for the case of a PV-battery system located in Rotterdam (shown in Figure 10) and in Valencia, with or without CO_2 taxation. Notably, the LCOE values found are much lower than the ones found for Rotterdam and the difference between the corresponding curves increases moving to the region of lower CO_2 emissions. This is because the installed PV power necessary to reach high electricity self-sufficiency decreases dramatically for the plant located in Valencia. Moreover, it is evident that the LCOE trend is flatter in this last case, especially in the scenario with the tax on the CO_2 emissions.

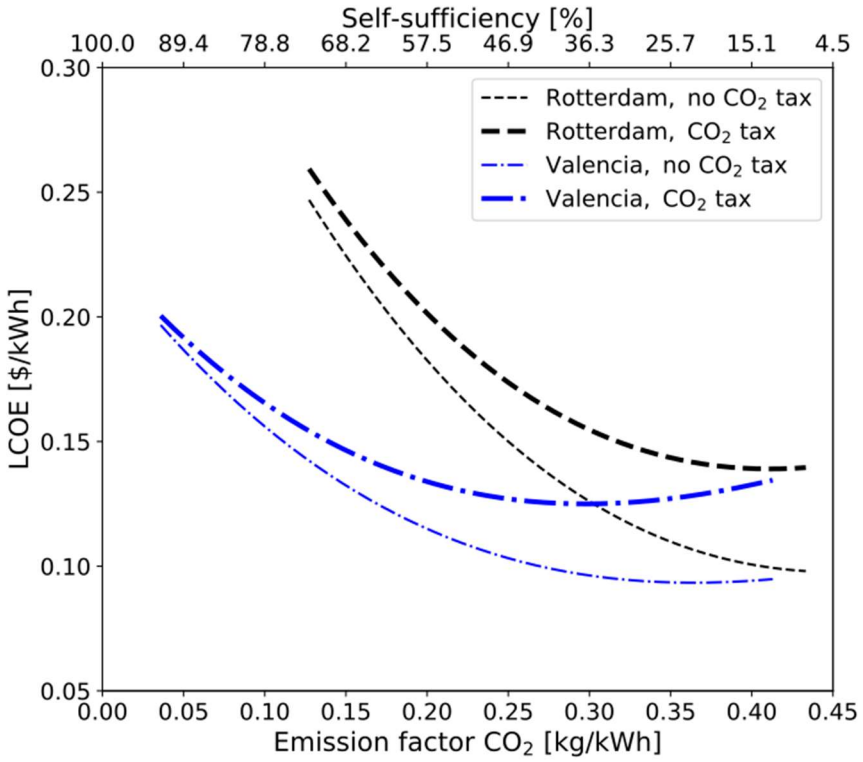

Figure 12. Lower envelopes of the scatter plots of LCOE [$/kWh] vs. the CO_2 emission factor [kg/kWh], varying $P_{PV,inst}/P_{demand}$ between 0.5 and 10 (step of 0.5) and $C_{battery}$ between 0 and 17.5h (step of 2.5h), for the case of a plant located in Rotterdam and in Valencia. Thinner lines: no taxation on the CO_2 emissions, thicker lines: taxation of 80€/ton_{CO2}.

The LCOE values calculated for the system in Valencia are employed as inputs for the two selected chains and the LBC_{tot} values (only the ones including the taxation on the CO_2 emissions) are reported vs. the CO_2 emissions in Figure 13. Both chains show a much flatter trend of LBC_{tot} vs. the specific CO_2 emissions, because of the flatter LCOE trend in the case of Valencia. It is remarkable the shift of both curves towards lower CO_2 emissions, since the self-sufficiency (fraction of self-generated electricity) reaches 92%, while in the Rotterdam case the maximum self-sufficiency was around 73%. Moreover, in this case, both chains result economically feasible in the whole range of LCOE, since LBC_{tot} is always lower than the threshold cost. This analysis shows the high potential of the proposed systems, which result economically competitive and able to guarantee a significant reduction of the CO_2 emissions. In fact, the CO_2 emissions go down to 0.77kg_{CO2}/m^3_{brine} in the case of the MED chain and to 1.26kg_{CO2}/m^3_{brine} in the case of the RO-MD chain. Thus, in both cases, an emission reduction higher than 90% compared to the current system is achieved.

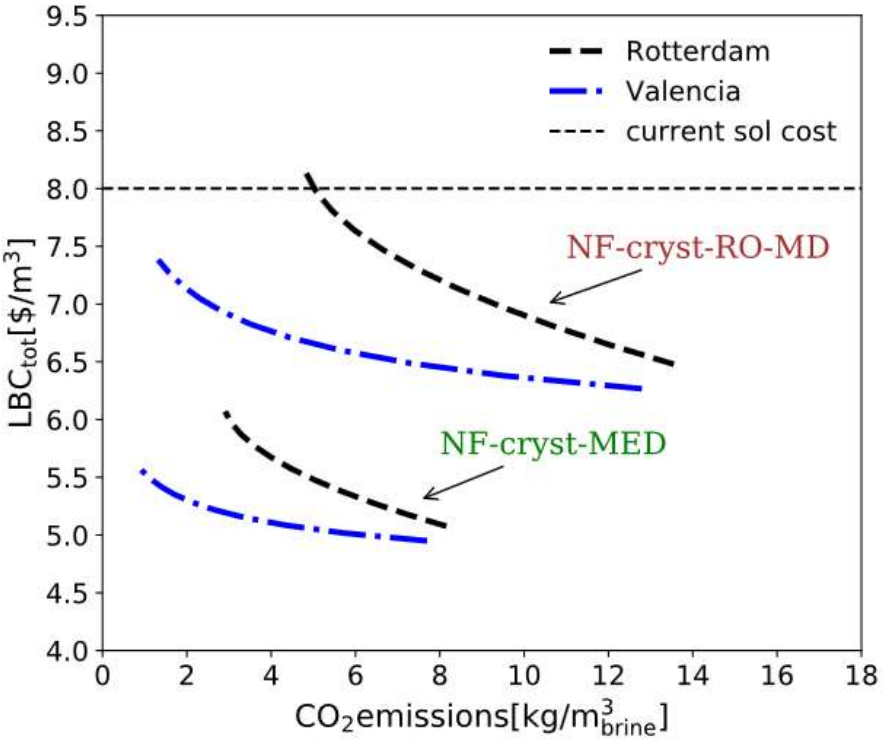

Figure 13. Comparison of the LBC_{tot} trends [$/$m^3_{brine}$] of the two chains (NF-cryst-MED and NF-cryst-RO-MD) vs. the CO_2 emission [kg/ m^3_{brine}], assuming CO_2 taxation of 80€/ton_{CO2}, for the case of a plant located in Rotterdam (case study, in black) and in Valencia, Spain (in blue).

4.3 Implications

We compared the global outputs obtained in the two scenarios, to highlight the implications of the proposed strategies in terms of economic feasibility and environmental impact. Figure 14 reports the LBC_{tot} and the CO_2 emissions per m^3 of brine. In particular, the current CO_2 emissions due to the fresh NaCl salt production are compared with the ones due to the chains' energy demand (i) when the electricity is taken from the grid and (ii) when the electricity is partially supplied by a PV-battery system, in the two different locations and with the maximum share of renewables at which the LBC_{tot} resulted below the threshold. The corresponding values of LBC_{tot} are compared with the current cost of the fresh regenerant solution. Notably, all systems ensure a reduction of the CO_2 emissions and a more competitive LBC_{tot} in comparison with the current system. The employment of renewable energy sources allows a net reduction of the CO_2 emissions, but the LBC_{tot} are higher than in scenario 1; conversely, the relatively low cost of the electricity from the grid leads to lower LBC_{tot} but the reduction of CO_2 emissions is less significant than in scenario 2.

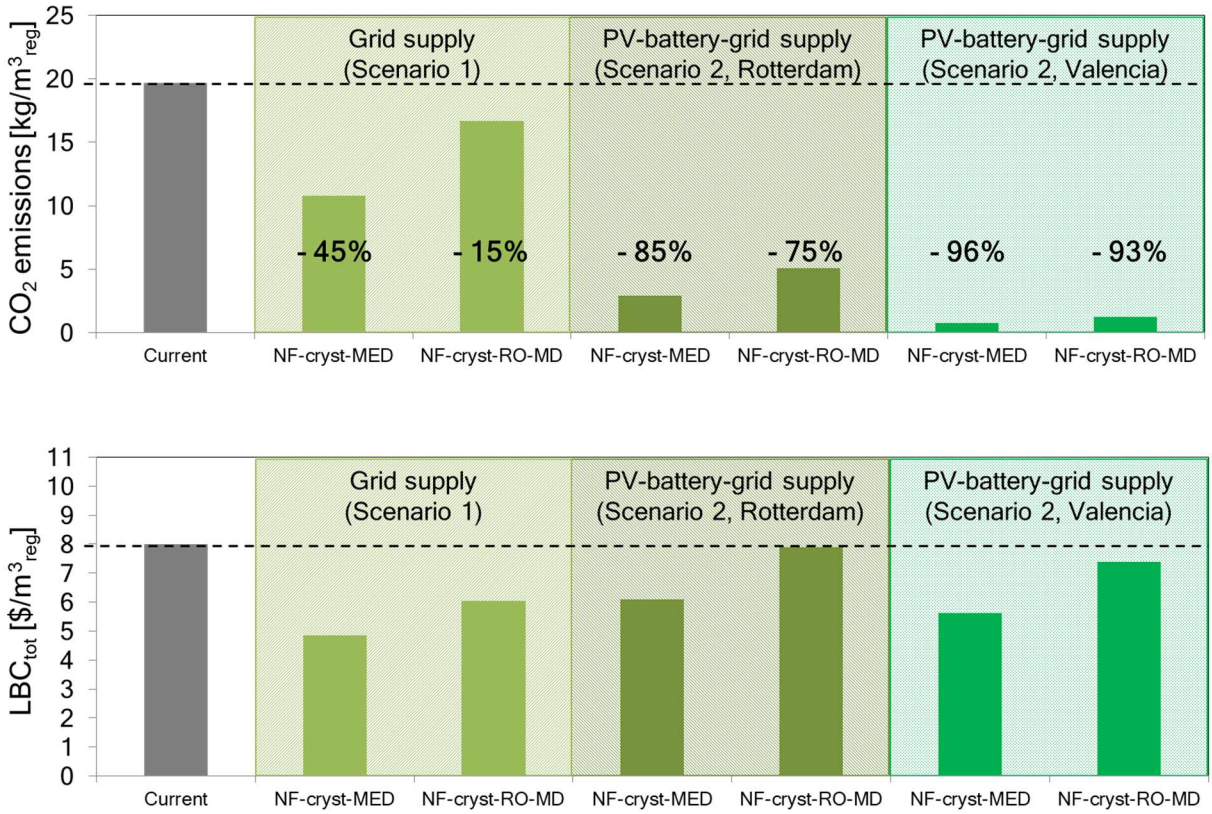

Figure 14. Values of CO_2 emissions per $m^3_{regenerant}$ (figure above) and the corresponding LBC_{tot} (figure below) for the current system and for the analysed scenarios. For scenario 2, LBC_{tot} refer to the cases with carbon tax and minimum emissions (maximum self-sufficiency). Q_{feed}=130m^3/h; waste heat, $Cost_{heat}$=0.01$/kWh$_{th}$.

5. Conclusions

This work presents an integrated methodological approach used to conduct a comprehensive analysis of different strategies to move towards Circular Economy in the water softening industry. These strategies aim (i) at recycling the effluent as reactant in the regeneration of IEX resins and (ii) at recovering valuable raw materials. Using the developed approach, for the first time, different concentration technologies and energy supply systems are proposed to identify the most economically convenient and environmentally friendly system to treat the wastewater. The proposed treatment chains include a pre-treatment step, composed of nanofiltration and crystallization, and a concentration step. Three alternative concentration steps are evaluated: MED, MD and the combination of RO and MD. For these, we set a common target concentration of the treated solution, which has then to be recycled to the industrial process. Therefore, the systems present the same circularity degree, which in turn corresponds to different costs and energy demand depending on the processes involved. The chains with RO-MD and with MED showed a wide range of feasible flow-rates and heat

costs. In particular, the RO-MD chain resulted more convenient at small scales for its lower investment costs, while the MED chain resulted more feasible at larger scales, for its lower energy requirements. Concerning the environmental impact of the two chains, the CO_2 emissions per m^3 of brine reusable as regenerant, were lower than those due to the production of the fresh regenerant, when electricity is taken from the grid. In particular, for a feed flow-rate of 130m^3/h, the two chains are economically feasible since the LBC_{tot} is equal to 4.6 and 6.4\$/m^3 for the MED and the RO-MD chain respectively (both lower that the current cost of the regenerant, i.e. 8\$/m^3). Also, they have lower carbon footprints, since the respective operational CO_2 emissions amount to 10.8 and 16.7$kg_{CO2}/m^3_{brine,}$ while the currently produced ones to 19.7kg_{CO2}/m^3_{brine}. The chain with MD only reported the worst results in terms of costs and CO_2 emissions, for the high MD thermal demand.

Furthermore, we investigated the possibility to couple the chains with a PV-battery system and we considered two locations: Rotterdam (The Netherlands, location of the real softening plant) and Valencia (Spain, for its high solar potential). A large decrease of the emissions was found: in Rotterdam, the CO_2 emission per m^3_{brine} resulted 75% and 85% lower than the current ones for the RO-MD and the MED chain, respectively and in Valencia, the reduction was higher than 90% for both chains. Moreover, the plants resulted economically feasible, even when the LCOE was more than two times the electricity cost from the grid.

Overall, the MED chain resulted more economically convenient and showed lower emissions in most cases, because of the lower energy requirements. However, the chain with RO-MD proved to be more feasible at lower scales and, in general, this system should be taken into account for its higher modularity and flexibility. Concluding, the NF-cryst-MED and NF-cryst-RO-MD chains should be regarded as valuable options for the implementation of a CE approach in the water softening industry.

Future works will investigate the other terms having an environmental impact, beyond the energy requirements of the treatment systems. The analysis will include the assessment of the CO_2 footprints due to the construction of the treatment units. Other future developments will consist in the application of the presented methodological approach to other case studies with different industrial effluents, to evaluate the most feasible and environmentally friendly strategy to treat and recycle the wastewater.

Acknowledgements

This work was funded by the ZERO BRINE project (ZERO BRINE–Industrial Desalination–Resource Recovery–Circular Economy)-Horizon 2020 programme, Project Number: 730390. www.zerobrine.eu.

Nomenclature

C	Concentration
$C_{battery}$	Capacity of the battery [h]
CAPEX	Capital Expenditure
CE	Circular Economy
$Cost_{El}$	Electricity cost [$/kWh]
$Cost_{Heat}$	Thermal energy cost [$/kWh]
Cryst	Crystallizer
DCMD	Direct Contact Membrane Distillation
$f_{CO2,emission}$	CO_2 emission factor [kg_{CO2}/kWh]
IEX	Ion Exchange resins
LBC	Levelized Brine Cost
LBC_{CAP}	Capital Levelized Brine Cost
LBC_{OP}	Operating Levelized Brine Cost
LCOE	Levelized Cost of Electricity
MD	Membrane distillation
MED	Multi-effect distillation
NF	Nanofiltration
OPEX	Operating Expenditure
P	Power [kW]
PV	Photovoltaic
Q	Flow rate [m^3/h]
RCE	Remote Component Environment
RO	Reverse osmosis
SD	Sustainable Development

Subscripts

Prim	primary energy
PV,inst	installed PV power

Bibliography

Abdelkader, S., F. Gross, D. Winter, J. Went, J. Koschikowski, S. U. Geissen, and L. Bousselmi. 2019. Application of direct contact membrane distillation for saline dairy effluent treatment: performance and fouling analysis. Environmental Science and Pollution Research **26**:18979–18992.

Al-Obaidani, S., E. Curcio, F. Macedonio, G. Diprofio, H. Alhinai, and E. Drioli. 2008. Potential of membrane distillation in seawater desalination: Thermal efficiency, sensitivity study and cost estimation. Journal of Membrane Science **323**:85-98.

Ali, A., J.-H. Tsai, K.-L. Tung, E. Drioli, and F. Macedonio. 2018. Designing and optimization of continuous direct contact membrane distillation process. Desalination **426**:97-107.

Bilińska, L., M. Gmurek, and S. Ledakowicz. 2017. Textile wastewater treatment by AOPs for brine reuse. Process Safety and Environmental Protection **109**:420-428.

Birnhack, L., O. Keller, S. C. N. Tang, N. Fridman-Bishop, and O. Lahav. 2019. A membrane-based recycling process for minimizing environmental effects inflicted by ion-exchange softening applications. Separation and Purification Technology **223**:24-30.

Boulding, K. E., and H. Jarrett. 1966. Essays from the sixth resources for the future forum on environmental quality in a growing economy.

Breyer, C., S. Afanasyeva, D. Brakemeier, M. Engelhard, S. Giuliano, M. Puppe, H. Schenk, T. Hirsch, and M. Moser. 2017. Assessment of mid-term growth assumptions and learning rates for comparative studies of CSP and hybrid PV-battery power plants.

Cardinali, A., S. Pati, F. Minervini, I. D'Antuono, V. Linsalata, and V. Lattanzio. 2012. Verbascoside, isoverbascoside, and their derivatives recovered from olive mill wastewater as possible food antioxidants. J Agric Food Chem **60**:1822-1829.

Cardona, C. A., J. A. Quintero, and I. C. Paz. 2010. Production of bioethanol from sugarcane bagasse: Status and perspectives. Bioresour Technol **101**:4754-4766.

Chandrasekara, N. P. G. N., and R. M. Pashley. 2015. Study of a new process for the efficient regeneration of ion exchange resins. Desalination **357**:131-139.

Chen, Y., J. R. Davis, C. H. Nguyen, J. C. Baygents, and J. Farrell. 2016. Electrochemical Ion-Exchange Regeneration and Fluidized Bed Crystallization for Zero-Liquid-Discharge Water Softening. Environ Sci Technol **50**:5900-5907.

Cipollina, A., M. Bevacqua, P. Dolcimascolo, A. Tamburini, A. Brucato, H. Glade, L. Buether, and G. Micale. 2014. Reactive crystallisation process for magnesium recovery from concentrated brines. Desalination and Water Treatment **55**:2377-2388.

Dow Water and Process Solutions. Filmtec Reverse Osmosis Membrane. Technical Manual.

EIA. 2019. Monthly Report of Natural Gas Purchases and Deliveries to Consumers.

El-Dessouky, H., and H. Ettouney. 1999. Multiple-effect evaporation desalination systems: thermal analysis. Desalination **125**:259-276.

Ellen MacArthur Foundation. 2013. Towards the Circular Economy-Economic and business rationale for an accelerated transition (part 1).

Eurostat. 2018. Which indicators are used to monitor the progress towards a circular economy?

Eurostat. 2019. Electricity prices for non-household consumers - bi-annual data (from 2007 onwards).

Fraunhofer ISE. 2015. Current and Future Cost of Photovoltaics. Long-term Scenarios for Market Development, System Prices and LCOE of Utility-Scale PV Systems. Agora Energiewende.

Gebel, J., and S. Yuce. 2008. An Engineer's Guide to Desalination. VBG PowerTech.

Geissdoerfer, M., P. Savaget, N. M. P. Bocken, and E. J. Hultink. 2017. The Circular Economy – A new sustainability paradigm? Journal of Cleaner Production **143**:757-768.

Geraldes, V., and A. M. Brites Alves. 2008. Computer program for simulation of mass transport in nanofiltration membranes. Journal of Membrane Science **321**:172-182.

Ghisellini, P., C. Cialani, and S. Ulgiati. 2016. A review on circular economy: the expected transition to a balanced interplay of environmental and economic systems. Journal of Cleaner Production **114**:11-32.

Giagnorio, M., A. Amelio, H. Grüttner, and A. Tiraferri. 2017. Environmental impacts of detergents and benefits of their recovery in the laundering industry. Journal of Cleaner Production **154**:593-601.

Gopinath, A., A. Bahurudeen, S. Appari, and P. Nanthagopalan. 2018. A circular framework for the valorisation of sugar industry wastes: Review on the industrial symbiosis between sugar, construction and energy industries. Journal of Cleaner Production **203**:89-108.

Gusmerotti, N. M., F. Testa, F. Corsini, G. Pretner, and F. Iraldo. 2019. Drivers and approaches to the circular economy in manufacturing firms. Journal of Cleaner Production **230**:314-327.

Harmelink, M., and L. Bosselaar. 2013. Allocating CO2 emissions to heat and electricity. Harmelink consulting.

Hitsov, I., L. Eykens, W. D. Schepper, K. D. Sitter, C. Dotremont, and I. Nopens. 2017. Full-scale direct contact membrane distillation (DCMD) model including membrane compaction effects. Journal of Membrane Science **524**:245-256.

Hitsov, I., K. D. Sitter, C. Dotremont, and I. Nopens. 2018. Economic modelling and model-based process optimization of membrane distillation. Desalination **436**:125-143.

Holkar, C. R., A. J. Jadhav, D. V. Pinjari, N. M. Mahamuni, and A. B. Pandit. 2016. A critical review on textile wastewater treatments: Possible approaches. J Environ Manage **182**:351-366.

International Energy Agency. 2018. World Energy Outlook 2018.

IPCC. 2006. 2006 IPCC Guidelines for National Greenhouse Gas Inventories. National Greenhouse Gas Inventories Programme, IGES, Japan.

Janeiro, L., and M. K. Patel. 2015. Choosing sustainable technologies. Implications of the underlying sustainability paradigm in the decision-making process. Journal of Cleaner Production **105**:438-446.

Kamali, R. K., A. Abbassi, S. A. Sadough Vanini, and M. Saffar Avval. 2008. Thermodynamic design and parametric study of MED-TVC. Desalination **222**:596-604.

Kesieme, U. K., N. Milne, H. Aral, C. Y. Cheng, and M. Duke. 2013. Economic analysis of desalination technologies in the context of carbon pricing, and opportunities for membrane distillation. Desalination **323**:66-74.

Labban, O., C. Liu, T. H. Chong, and J. H. Lienhard V. 2017. Fundamentals of low-pressure nanofiltration: Membrane characterization, modeling, and understanding the multi-ionic interactions in water softening. Journal of Membrane Science **521**:18-32.

Li, J., S. Koner, M. German, and A. K. SenGupta. 2016. Aluminum-Cycle Ion Exchange Process for Hardness Removal: A New Approach for Sustainable Softening. Environ Sci Technol **50**:11943-11950.

Liu, J., S. Chen, H. Wang, and X. Chen. 2015. Calculation of Carbon Footprints for Water Diversion and Desalination Projects. Energy Procedia **75**:2483-2494.

Lopez, J., M. Reig, O. Gibert, and J. L. Cortina. 2019. Integration of nanofiltration membranes in recovery options of rare earth elements from acidic mine waters. Journal of Cleaner Production **210**:1249ß1260.

Malek, A., M. N. A. Hawlader, and J. C. Ho. 1996. Design and economics of RO seawater desalination. Desalination **105**:245-261.

Man, Y., W. Shen, X. Chen, Z. Long, and M.-N. Pons. 2017. Modeling and simulation of the industrial sequencing batch reactor wastewater treatment process for cleaner production in pulp and paper mills. Journal of Cleaner Production **167**:643-652.

Mezher, T., H. Fath, Z. Abbas, and A. Khaled. 2011. Techno-economic assessment and environmental impacts of desalination technologies. Desalination **266**:263-273.

Micari, M., A. Cipollina, A. Tamburini, M. Moser, V. Bertsch, and G. Micale. 2019a. Combined membrane and thermal desalination processes for the treatment of ion exchange resins spent brine. Applied Energy **254**.

Micari, M., M. Moser, A. Cipollina, B. Fuchs, B. Ortega-Delgado, A. Tamburini, and G. Micale. 2019b. Techno-economic assessment of multi-effect distillation process for the treatment and recycling of ion exchange resin spent brines. Desalination **456**:38-52.

Mirabella, N., V. Castellani, and S. Sala. 2014. Current options for the valorization of food manufacturing waste: a review. Journal of Cleaner Production **65**:28-41.

Moser, M., F. Trieb, T. Fichter, J. Kern, and D. Hess. 2014. A flexible techno-economic model for the assessment of desalination plants driven by renewable energies. Desalination and Water Treatment:1-15.

Nadeem, K., G. T. Guyer, B. Keskinler, and N. Dizge. 2019. Investigation of segregated wastewater streams reusability with membrane process for textile industry. Journal of Cleaner Production **228**:1437-1445.

Ortega-Delgado, B., L. García-Rodríguez, and D.-C. Alarcón-Padilla. 2017. Opportunities of improvement of the MED seawater desalination process by pretreatments allowing high-temperature operation. Desalination and Water Treatment **97**:94-108.

Papapetrou, M., A. Cipollina, U. La Commare, G. Micale, G. Zaragoza, and G. Kosmadakis. 2017. Assessment of methodologies and data used to calculate desalination costs. Desalination **419**:8-19.

Qtaishat, M., T. Matsuura, B. Kruczek, and M. Khayet. 2008. Heat and mass transfer analysis in direct contact membrane distillation. Desalination **219**:272-292.

Roy, Y., M. H. Sharqawy, and J. H. Lienhard. 2015. Modeling of flat-sheet and spiral-wound nanofiltration configurations and its application in seawater nanofiltration. Journal of Membrane Science **493**:360-372.

Saidani, M., B. Yannou, Y. Leroy, F. Cluzel, and A. Kendall. 2019. A taxonomy of circular economy indicators. Journal of Cleaner Production **207**:542-559.

Sarayu, K., and S. Sandhya. 2012. Current technologies for biological treatment of textile wastewater--a review. Appl Biochem Biotechnol **167**:645-661.

Sassanelli, C., P. Rosa, R. Rocca, and S. Terzi. 2019. Circular economy performance assessment methods: A systematic literature review. Journal of Cleaner Production **229**:440-453.

Sedivy, V. M. 2006. Environmental balance of salt production speaks in favour of solar saltworks.*in* 1st International Conference on the Ecological Importance of Solar Saltworks, Santorini.

Suárez-Eiroa, B., E. Fernández, G. Méndez-Martínez, and D. Soto-Oñate. 2019. Operational principles of circular economy for sustainable development: Linking theory and practice. Journal of Cleaner Production **214**:952-961.

Turek, M., P. Dydo, and R. Klimek. 2008. Salt production from coal-mine brine in NF — evaporation — crystallization system. Desalination **221**:238-243.

Turton, R., R. C. Bailie, W. B. Whiting, J. A. Shaeiwity, and D. Bhattacharzza. 2012. Analysis, Synthesis and Design of Chemical Processes. Prentice Hall.

U.S. Department of the Interior. 2017. Mineral Commodity Summaries - U.S. Geological Survey.

Van der Bruggen, B., K. Everaert, D. Wilms, and C. Vandecasteele. 2001. Application of nanofiltration for removal of pesticides, nitrate and hardness from ground water: rejection properties and economic evaluation. Journal of Membrane Science **193**:239-248.

Vince, F., F. Marechal, E. Aoustin, and P. Bréant. 2008. Multi-objective optimization of RO desalination plants. Desalination **222**:96-118.

Wilf, M., and C. Bartels. 2005. Optimization of seawater RO systems design. Desalination **173**:1-12.

Winter, D., J. Koschikowski, and M. Wieghaus. 2011. Desalination using membrane distillation: Experimental studies on full scale spiral wound modules. Journal of Membrane Science **375**:104-112.

World Commission on Environment and Development. 1987. Our Common Future.

Zhijun, F., and Y. Nailing. 2007. Putting a circular economy into practice in China. Sustainability Science **2**:95-101.

Zhou, D., L. Zhu, Y. Fu, M. Zhu, and L. Xue. 2015. Development of lower cost seawater desalination processes using nanofiltration technologies — A review. Desalination **376**:109-116.